Published OnlineFirst June 11, 2014; DOI: 10.1158/1078-0432.CCR-13-1559

antibodies were incubated following Ventana's instruction and the antibody product recommendation. The intensity of phosphor-Src expression was scored from 0–3 (0 = no expression, 1 = weak expression, 2 = moderate expression, and 3 = high expression), while the cellularity was scored from 0–3 (0 = 0%, 1 = 1-33%, 2 = 34-66%, and 3 = >66%). The H scores formed by intensity of immunoactivity timing cellularity were stratified as low (0–2), intermediate (3–4), and high (6–9).

MET-pY100 proximity ligation and total MET immunofluorescence

Slides containing 5-μm sections were rehydrated through xylene and graded alcohols. Heat-induced epitope retrieval was carried out in Tris-EDTA (pH 9) in a pressure cooker for 20 minutes and then allowed to cool for 20 minutes. Nonspecific binding was blocked by incubation with 1.5% BSA, and primary antibodies were incubated overnight in 1.5% BSA-PBST.

For proximity ligation, antibodies were rabbit anti-MET (clone D1C2, Cell Signaling Technology) and mouse anti-pY100 (Cell Signaling Technology). PLA probes were anti-rabbit (-) and anti-mouse (+) and were incubated for 1 hour in 0.15% BSA/PBST. Detection was carried out using the DuoLink in situ PLA Far Red kit (O-Link Biosciences, Uppsala, Sweden). AlexaFluor 488-conjugated anti-cytokeratin was used to demarcate epithelial regions (clone AE1/AE3, eBiosciences).

For immunofluorescence, antibodies were rabbit anti-MET (clone D1C2, Cell Signaling Technology) and detected via AlexaFluor 647-labeled anti-rabbit secondary antibodies (Invitrogen). Murine pan-cytokeratin (clone AE1/AE3, Dako) was used to demarcate epithelial regions (tumor mask) and detected via AlexaFluor 555-labeled anti-mouse secondary antibodies (Invitrogen). Images were acquired on a PM2000.

Statistical methods

Anderson-Darling statistics and normal curves were examined to assess whether tumor measurements were normally distributed. A square-root transformation was performed on the tumor measurements to make them approximately normal. ANOVA test was used to assess whether there was a statistically significant difference on tumor sizes measured across treatment groups at each time point. Tukey-Kramer method was used to perform all pairwise group comparisons. All statistical analyses were performed using SAS (version 9.2; SAS Institute; Cary, NC).

Results

Chronic gefitinib exposure of PC9 cells generates stable cell-autonomous resistance to EGFR-TKIs with T790M

After generation of PC9GR cells, we identified single-cell clones of PC9GR cells that were highly resistant to erlotinib (Supplementary Fig. S1A). Although PC9GR cells are partially sensitive to the irreversible EGFR-TKI CL387,785 as expected from a previous report (8), IC_{50} for CL387,785 was 100-fold increased compared with parent PC9 cells (Supplementary Fig. S1A). This resistance was stable as it was not reversed by culturing PC9GR cells for up to 6 months in gefitinib-free medium (data not shown). PC9GR cells acquired T790M while retaining exon 19 E746-A750, as determined by both direct DNA sequencing and PCR-invader assay (Supplementary Fig. S2A). In addition, we did not find *MET* amplification by FISH analysis in PC9GR cells (Supplementary Fig. S2B), which is another mechanism of acquired EGFR-TKI resistance in NSCLC (28). Erlotinib still has partial inhibitory effects on EGFR phosphorylation in PC9GR cells (Supplementary Fig. S1B), consistent with prior studies that T790M typically emerges as a minor population and resistant cells retain drug-sensitive alleles (8, 33). However, erlotinib could not completely inhibit downstream pAkt and pErk in PC9GR cells, consistent with resistance to EGFR-TKIs in the presence of T790M (Supplementary Fig. S1B).

System-level comparison of tyrosine phosphorylation identifies common RTK pathways associated with erlotinib resistance

We hypothesized that erlotinib-resistant PC9GR cells could collect additional mechanisms of resistance through acquired alterations in tyrosine kinase signaling that could collaborate with T790M to codrive resistance to EGFR-TKI. We therefore profiled tyrosine kinase signaling by charting tyrosine phosphorylated peptides in PC9 and PC9GR cells. As shown in our schema (Fig. 1), tryptic peptides were derived from cellular protein lysates and enriched with anti-phosphotyrosine (pTyr) antibodies followed by identification and quantification using liquid chromatography coupled with tandem mass spectrometry (LC/MS-MS; refs. 32, 34). Changes in peptides in PC9GR cells were identified and compared with PC9 cells, thus allowing us to determine additional changes beyond T790M that could be codrivers of TKI resistance. We perturbed EGFR-driven signaling in erlotinib-sensitive PC9 and erlotinib-resistant PC9GR cells to identify EGFR-dependent pathways/networks and potential pathways/networks independent of EGFR signaling that could play a role in EGFR-TKI resistance. After 1-hour erlotinib treatment, cell pellets were collected and pTyr peptides were identified in untreated and treated PC9 and PC9GR cells. Changes in peptides were identified compared with control vehicle-treated cells in each of the two cell lines. We hypothesized that this approach would identify downstream signaling events driven by mutated EGFR but could also potentially identify proteins or pathways activated by TKI or unaltered by TKI that could, under the correct circumstances, potentiate drug resistance. In total, between the two cell lines, we identified 403 pTyr peptides corresponding to 265 unique phosphoproteins. Examples of extracted ion chromatograms for pTyr peptides corresponding to EGFR and MET are shown in Supplementary Figs. S3 and S4.

We next compared changes in pTyr abundance between PC9 and PC9GR cells (Fig. 2A; Supplementary Table S1). We found 110 unique pTyr peptides (76 proteins) that were

Published OnlineFirst June 11, 2014; DOI: 10.1158/1078-0432.CCR-13-1559

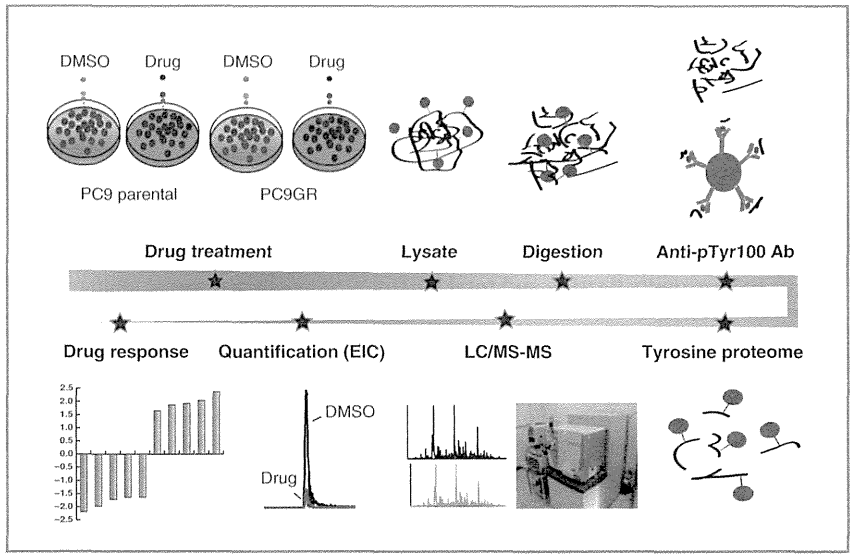

Figure 1. Phosphoprotein network associated with mutant EGFR and T790M tyrosine kinase signaling. Workflow of quantitative phosphoproteomics analysis. EIC, extracted ion chromatography (used to quantify peptide abundance for each of the identified tyrosine-containing peptides).

more abundant in the PC9GR cells, whereas 77 unique pTyr peptides (55 proteins) were less abundant in PC9GR cells than in PC9 cells. Compared with PC9 cells, PC9GR cells demonstrated increased amounts of pTyr peptides corresponding to numerous RTKs, some of which could be potential codrivers of resistance in PC9GR cells under the correct environmental circumstances. We observed a clear subnetwork characterized by hyperactive MET signaling (Fig. 2A, right) despite the lack of *MET* gene amplification. We observed nearly 11-fold more MET pTyr peptides in PC9GR than in PC9 cells. Similarly, we observed nearly >10-fold more pTyr peptides corresponding to ROR1 or neurotrophic tyrosine kinase receptor related-1 (pTyr-789, ~13-fold; pTyr-828, ~34-fold). ROR1 is a pseudokinase that cooperates with MET to promote tumorigenesis (35). Tyrosine phosphorylation of the MET adaptor proteins Gab1 and Gab2 were also more abundant in PC9GR cells.

In addition, pTyr peptides corresponding to the AXL RTK were increased approximately 8-fold in PC9GR cells. AXL upregulation has recently been shown to be a mechanism of acquired resistance of lung cancer cells to EGFR-TKI (36). Finally, increased abundance of multiple peptides corresponding to IRS2 (pTyr-675, 4.97-fold; pTyr-598, 5.47-fold; pTyr-823, 9.55-fold; pTyr-653, 19.93-fold; and pTyr-742, 21.29-fold), an adaptor protein linking insulin and insulin-like growth factor (IGF) signaling to PI3K signaling, was observed in PC9GR cells compared with parent PC9 cells. This suggested that either more insulin or IGF signaling exists in these cells or more IRS2 protein is expressed. We confirmed higher levels of tyrosine-phosphorylated MET and AXL in PC9GR than in PC9 cells and also found more total IRS2 protein in PC9GR than in PC9 cells (Fig. 2B). Despite the increased levels of MET signaling, we found minimal effects of combined MET-TKI (PHA665752) and EGFR-TKI (erlotinib or irreversible CL387,785) in PC9GR cells (Fig. 2C). While MET signaling is hyperactivated, in this context, it is not responsible for affecting cell survival.

To examine whether changes of MET, IRS2, or AXL are driven specifically by T790M, we examined phosphorylation of these molecules in lung cancer cell lines (HCC4006 and HCC827) engineered to express an exon 19 E746-A750 + T790M allele. (Fig. 2B). We observed less pMET, less total MET, slightly more abundant pAXL, and similar total AXL in HCC4006-T790M cells compared with parent HCC4006 cells. We found equivalent pMET and total MET, less pAXL and equivalent total AXL in HCC827-T790M cells compared with parent HCC827 cells. The levels of IRS2 protein were unchanged across these HCC4006 and HCC827 cell lines unlike in PC9 and PC9GR cells. These results suggest that changes of MET, IRS2, or AXL are not dependent on *EGFR*-T790M but rather are likely to occur on a cell by cell basis.

Perturbations by EGFR-TKI identify downstream proteins and proteins involved in adaptive and microenvironment-derived responses

We next compared alterations in pTyr peptide abundance in both cell lines following erlotinib exposure (Supplementary Table S1). We identified pTyr peptides with >1.5-fold change differences from control ($P < 0.05$). In PC9 cells, we observed 31 less abundant and 45 more abundant unique pTyr peptides following 1 hour of erlotinib treatment (Fig. 3A). As expected, PC9GR cells displayed a more blunted response to erlotinib than PC9 cells; nonetheless, we did observe congruent changes in most pTyr peptides, thus increasing our confidence that these pTyr peptides and pathways are downstream of mutant EGFR given the expected biologic responses with cells harboring T790M mutations. Among the reduced pTyr peptides, we observed MK01, SHC1, GAB1, EGFR, and ERBB3 consistent with their known roles in ERBB signaling. Interestingly, we also observed reductions in peptides corresponding to Ras

Published OnlineFirst June 11, 2014; DOI: 10.1158/1078-0432.CCR-13-1559

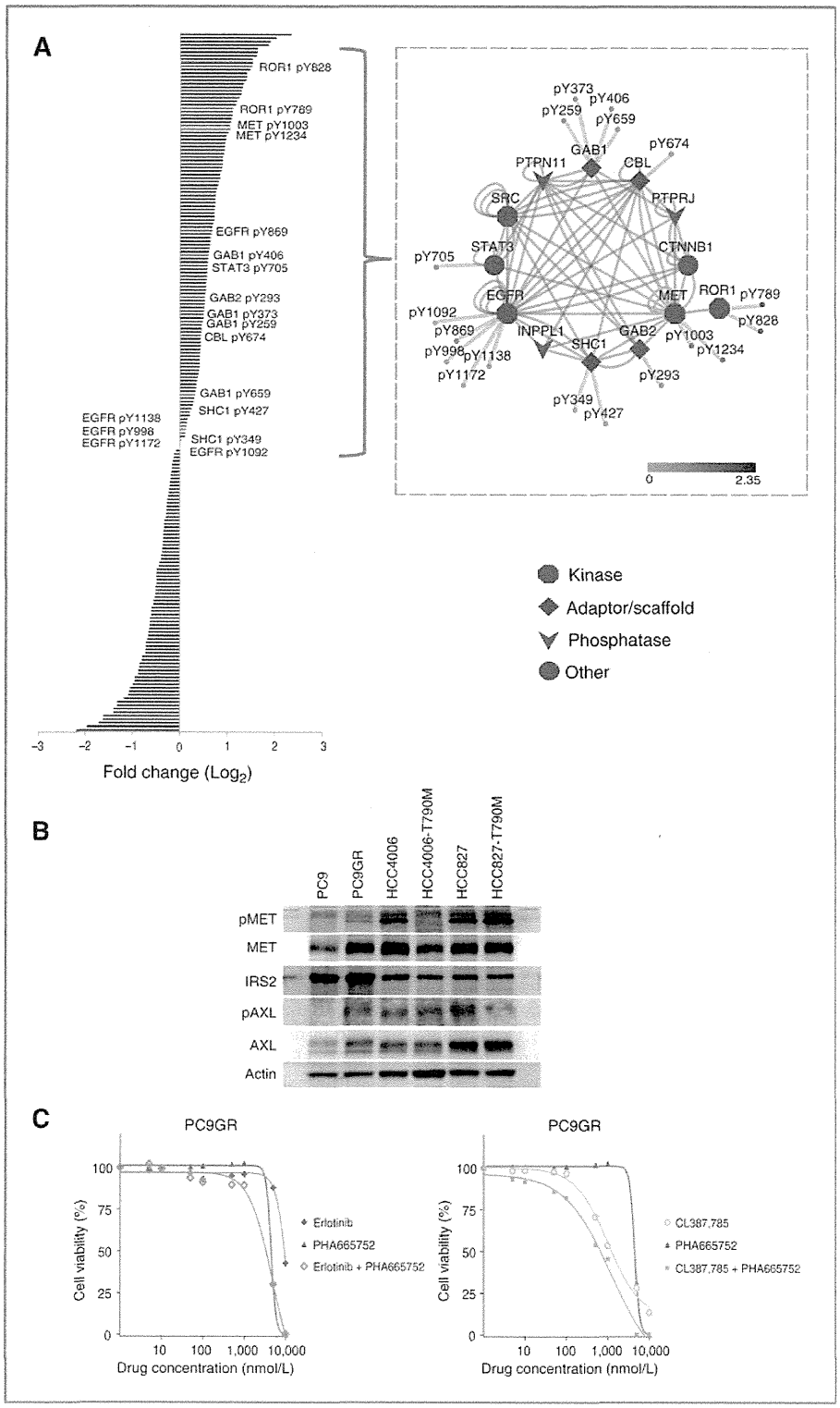

Published OnlineFirst June 11, 2014; DOI: 10.1158/1078-0432.CCR-13-1559

signaling, including SYGP1 or SynGAP, which can affect ERK and p38 MAPK functions in neurons (37, 38). Tyrosine-phosphorylated Rab7A (also known as Ras-related protein Rab-7a) was likewise reduced by erlotinib and has been linked to EGFR trafficking in endosomes (39).

Interestingly, we observed that nearly equal amounts of pTyr peptides were increased by erlotinib compared with peptides reduced by erlotinib (45 up and 31 down in PC9; 26 up and 30 down in PC9GR). We found more abundant pTyr peptides for IRS2, MET, YES, AXL, FAK, ERBB2, and BRK (PTK6) following erlotinib treatment, and this pattern was consistent across both PC9 and PC9GR cells (Fig. 3B). We hypothesized that the increased levels of RTK identified through our approach could cooperate with exogenous ligands and promote EGFR-TKI resistance. Recent studies have highlighted the ability of growth factor ligands to promote resistance to targeted agents (23–25). We therefore tested if the increased pTyr in key RTK could cooperate with growth factor ligands to drive resistance to EGFR-TKI. We incubated PC9 and PC9GR cells with cognate ligands corresponding to the upregulated RTK in PC9GR, including IGF1, hepatocyte growth factor (HGF), and GAS6 (the ligand for AXL RTK), and determined the effects on erlotinib sensitivity in PC9 cells and afatinib sensitivity in PC9GR cells (Fig. 3C). Interestingly, HGF and IGF but not GAS6 had protective effects on both PC9 cells exposed to erlotinib and PC9GR cells exposed to afatinib. In PC9 cells, the shift in IC_{50} was rather modest; however, in PC9GR cells, the effect was more dramatic. This shift pattern was consistent between both cell lines, with HGF having more of an effect than IGF1, whereas no effect was seen with activation of AXL by GAS6 in these cells. Using Western blotting, we examined the effects of these ligands on EGFR signaling with or without EGFR-TKI in both PC9 and PC9GR cells. HGF activated pMET in both PC9 and PC9GR cells (Supplementary Fig. S5A and S5B). This HGF-induced activation of pMET and downstream pAkt and pErk were not inhibited by erlotinib in PC9 or by afatinib in PC9GR cells (Supplementary Fig. S5A and S5B). These results also suggest that MET activation in PC9 and PC9GR cells is not dependent on EGFR signaling. On the other hand, we did not observe clear ligand-dependent activation of corresponding RTKs or sustained activation of pAkt and pErk in the presence of EGFR-TKIs in IGF1-induced or Gas6-induced PC9 and PC9GR cells (Supplementary Fig. S5C–S5F). These results are consistent with our data showing that IGF1 and Gas6 had less rescue effects compared with HGF in these cells (see Fig. 3C). These results suggest that altered RTK identified by phosphoproteomics can be codrivers of resistance under specific environmental circumstances. Furthermore, the increased levels of multiple RTKs in response to erlotinib suggest innate priming of RTK, where RTKs are primed to cooperate with growth factor ligands through intracellular mechanisms.

Afatinib combined with dasatinib inhibits EGFR signaling more efficiently than either agent alone in TKI-resistant NSCLC cells with T790M

We reexamined our data for pTyr peptides that were not perturbed by EGFR-TKI and were not different between the PC9 and PC9GR cell lines. We hypothesized that this analysis may uncover parallel signaling pathways that cooperate with EGFR to maintain cellular growth and/or survival. We identified 31 proteins that fulfilled this criterion, including multiple SFKs as well as CSK, PKCD, MAPK3, PIK3R2, SYK, TNK2, EPHB2, EPHA4, FAK, and PTK2B. We observed no changes in pTyr peptides corresponding to SFKs, including the pTyr peptide LIEDNEyTAR corresponding to the common autocatalytic site in c-SRC, YES, and FYN, following EGFR-TKI, suggesting this as an EGFR-independent pathway. We linked SFK proteins to other proteins found in our entire dataset through interaction databases (Fig. 4A), identifying a large group of proteins ($N = 28$) with reported interactions with SFK proteins (gray circles) that were also unchanged by erlotinib. In addition, we identified potential interactions between SFK and proteins either altered by erlotinib (gray parallelogram and diamond) or altered in PC9GR compared with PC9 cells (gray V and diamond). For example, SRC can cooperate with EGFR, MET, ERBB3, SHC1, CBL, and STAT3 signaling nodes (gray parallelogram) that we previously identified as being altered by erlotinib and different between PC9 and PC9GR cells.

On the basis of this observation, we hypothesized that cotargeting SFKs and EGFR T790M with dasatinib and afatinib, respectively, may produce additive or synergistic anti-tumor effects. Furthermore, our previous studies suggested that the antitumor effects of dasatinib are mediated in part by direct EGFR inhibition that is mitigated by gain of T790M in *EGFR* (32). However, these studies also suggested that irreversible EGFR-TKIs combined with dasatinib could

Figure 2. Phosphoproteins associated with T790M-mediated resistance. A, connectivity of MET protein was determined using protein–protein interaction databases to better aid in visualizing differentially expressed proteins that may be associated with PC9GR cells. The left histograph shows change of pTyr sites in PC9GR cells compared with in PC9 cells. The fold change ($P < 0.05$, fold change > 1.5) of all tyrosine peptides were presented in $\log_2$ scale. Red bar shows the tyrosine phosphosites of MET network proteins in PC9GR cells. Right, the MET network. Statistically decreased or increased pTyr peptides were input into Cytoscape 2.8.3, and protein–protein interactions were identified using InnateDB based on molecular interactions and functional relations from public sources. Shapes reflect types of proteins shown in figure. Pink circle represents the pTyr peptides significantly different between PC9 and PC9GR cells and different between erlotinib-treated and control cells ($P < 0.05$; fold change >1.5). Color scale corresponds to fold change in Log2 scale. The yellow lines represent the direct interaction with MET. B, Western blotting of selected proteins in PC9, PC9GR, HCC4006, HCC4006-T790M, HCC827, HCC827-T790M cells. Membranes were blotted with pTyr 1234/1235 MET, total MET, pTyr 702 AXL, total AXL, and total IRS2 antibodies in PC9, PC9GR, HCC4006, HCC4006-T790M, HCC827, HCC827-T790M cells with actin confirming equal protein loading. C, PC9GR cells were treated for 72 hours with increasing concentrations of erlotinib alone, CL387,785 alone, PHA665752 alone, erlotinib + PHA665752, or CL387,785 + PHA665752. Data generated by cell viability assay (CellTiter-Glo) are expressed as a percentage of the value for untreated cells. Determinations were done in triplicate. Please view online version for full details.

Published OnlineFirst June 11, 2014; DOI: 10.1158/1078-0432.CCR-13-1559

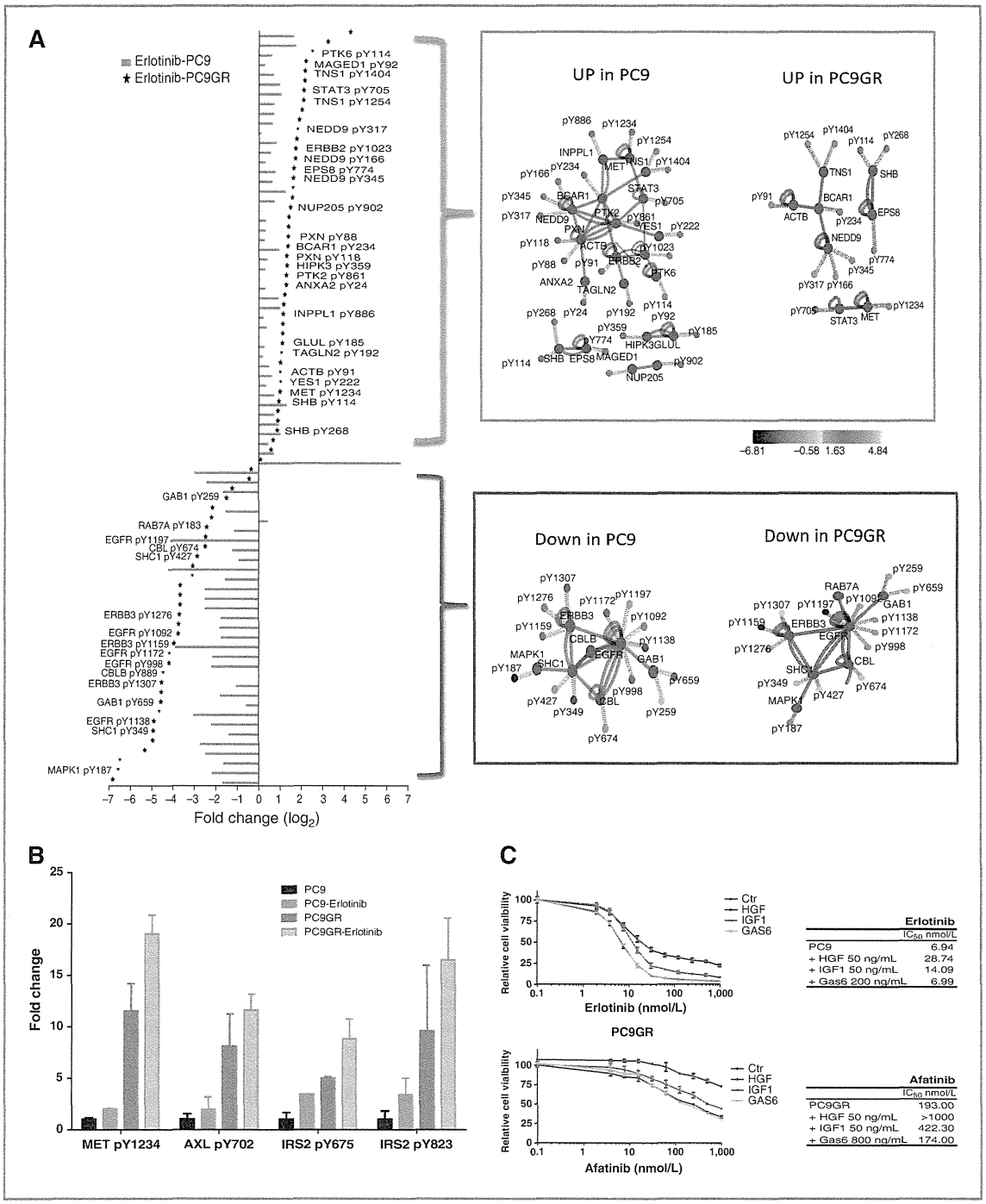

Erlotinib	IC_{50} nmol/L
PC9	6.94
+ HGF 50 ng/mL	28.74
+ IGF1 50 ng/mL	14.09
+ Gas6 200 ng/mL	6.99

Afatinib	IC_{50} nmol/L
PC9GR	193.00
+ HGF 50 ng/mL	>1000
+ IGF1 50 ng/mL	422.30
+ Gas6 800 ng/mL	174.00

Figure 3. Erlotinib perturbations in PC9 and PCGR cell lines. A, effects of erlotinib on tyrosine containing phosphoproteomes in PC9 and PC9GR cell lines. Left, erlotinib-induced changes ($P < 0.05$; fold change >1.5) of pTyr sites in PC9 (bars) and PC9GR (*) cells. Four subnetworks were created within different catalog proteins (blue circle) based on increased or decreased pTyr sites in PC9 and PC9GR cells. Color scale represents the fold change of each pTyr site. B, pTyr peptide abundance measured by EIC across erlotinib-treated PC9 and PC9GR cells for MET, AXL, and IRS2 pTyr peptides. Y-axis indicates fold change above PC9 untreated pTyr abundance. C, PC9 or PC9GR cells were seeded in 96-well plates for 24 hours and then exposed to HGF or IGF1 (50 ng/mL) or GAS6 (200 ng/mL) and concomitantly exposed to increasing concentrations of relevant kinase inhibitor. After 72 hours, cell viability was assessed. IC_{50} was calculated for each condition. Please view online version for full details.

Published OnlineFirst June 11, 2014; DOI: 10.1158/1078-0432.CCR-13-1559

inhibit EGFR T790M. Thus, we examined the effects of erlotinib, afatinib, dasatinib, or combined afatinib and dasatinib on EGFR signaling in PC9GR and H1975 cells, both resistant cell lines against EGFR-TKI because of T790M (Fig. 4B). In both cell lines, erlotinib inhibited neither EGFR nor SFKs, and no complete suppression of pAkt and pErk (both essential downstream molecules of EGFR) was observed. We found that afatinib could inhibit pEGFR; however, SFKs were again unaltered. These results with erlotinib and afatinib are consistent with our pTyr mass spectrometry results that detected no changes in pTyr SFKs following erlotinib exposure. We also found that combining afatinib and dasatinib resulted in more efficient inhibition of pAkt and pErk in PC9GR and H1975 cells than each agent alone, suggesting that SFKs are cosignals related to EGFR T790M and that irreversible EGFR-TKIs combined with SFKs more efficiently block EGFR signaling in NSCLC cells harboring T790M.

Afatinib combined with dasatinib effectively inhibits cell growth and significantly increases apoptotic cells in TKI-resistant NSCLC cells with T790M

Given that the combination of afatinib and dasatinib efficiently inhibited EGFR signaling in NSCLC cells harboring T790M, we examined the effects of this combination on cell proliferation and apoptosis in PC9GR and H1975 cells. We found reduced IC_{50} levels in PC9GR and H1975 cells versus either agent alone (Fig. 4C; Supplementary Tables S2 and S3). We examined the effects of combining afatinib plus dasatinib in other NSCLC cells with T790M (HCC4006-T790M and HCC827-T790M cells), cells with TKI-sensitive *EGFR* mutation only (PC9, HCC4006, and HCC827 cells), and cells with wild-type EGFR (H460, A549, and H1299 cells). We observed reduced IC_{50} for afatinib plus dasatinib versus either agent alone in HCC4006-T790M and HCC827-T790M cells (Supplementary Fig. S6), whereas curves for this combination were mostly overlapped with those for afatinib or dasatinib alone in PC9, HCC4006, and HCC827 cells with TKI-sensitive *EGFR* mutation only (Supplementary Fig. S7) or H460, A549, and H1299 cells with wild-type *EGFR* (Supplementary Fig. S8). We also found that dasatinib combined with CL387,785, another irreversible EGFR-TKI, reduced IC_{50} versus either agent alone in PC9GR cells (Supplementary Fig. S9). Furthermore, we also detected more apparent PARP cleavage when agents were combined than when used alone or when cells were erlotinib treated (see Fig. 4B). Similar to results with afatinib, when we examined the effects of combined dasatinib with WZ4002, another T790M-specific EGFR-TKI (40), IC_{50} was reduced versus when agents were used alone (Fig. 4D; Supplementary Tables S2 and S3).

Rescue experiments revealed that dasatinib enhanced antitumor effects of afatinib by inhibition of SRC and FYN

Although our clustering approach and dasatinib results strongly implicated SFKs as the key target, we examined this in more detail given the extensive promiscuousness of dasatinib. Using dasatinib-insensitive alleles expressed in lentiviral vectors, we investigated whether dasatinib-resistant forms of key SFKs could rescue effects of dasatinib (32). To test which SFK is critical as a dasatinib target in NSCLC cells harboring T790M when combined with afatinib, we infected cells with lentivirus expressing either wild-type kinases or kinase alleles with drug-resistant gatekeeper mutations of SFKs (SRC, LYN, FYN, and FRK) and examined cell viability in response to increasing concentrations of dasatinib plus afatinib (Fig. 4E). Our results show that SRC and FYN were able to rescue PC9GR cells from dasatinib plus afatinib. However, no effects were observed with LYN and FRK, suggesting that SRC and FYN are essential SFKs as dasatinib targets in NSCLC cells with T790M.

Dasatinib enhances the antitumor activity of afatinib *in vitro* and *in vivo*

To evaluate more formally whether our combination effects were because of additional cell death, we measured caspase-3–positive cells following TKI treatment (Fig. 5A). In PC9GR cells, both erlotinib and dasatinib had no effects on apoptosis, but the combination had modest effects. Afatinib led to more apoptosis, which was further increased when combined with dasatinib. Similar effects of afatinib plus dasatinib on apoptosis were observed in HCC4006-T790M and HCC827-T790M cells (Supplementary Fig. S10). WZ4002 also induced apoptosis as a single agent, which was potentiated when combined with dasatinib. In H1975 cells, similar effects were observed, with dasatinib increasing apoptosis when added to afatinib and WZ4002. These results indicate that Src inhibitors enhance antiproliferative and proapoptotic effects of irreversible or T790M-selective EGFR-TKIs in NSCLC cells with T790M.

We hypothesized that the enhanced apoptosis with combined afatinib and dasatinib would translate into improved *in vivo* effects on tumor growth. We examined the antitumor effects of this combination in mouse xenograft models with PC9GR cells. As single agents, afatinib (10 mg/kg) or dasatinib (15 mg/kg) had modest effects on inhibiting tumor growth in PC9GR xenografts; however, when combined, we observed significantly greater inhibition of growth, including tumor regression consistent with our apoptosis results (Fig. 5B). These results demonstrate that Src inhibitors effectively enhance antitumor effects of irreversible EGFR-TKI in gefitinib-resistant NSCLC xenografts with T790M, providing a rationale to evaluate this strategy in patients with NSCLC who have acquired EGFR-TKI resistance related to T790M.

Tyrosine phosphoproteomes in lung adenocarcinoma samples with TKI-sensitive *EGFR* mutations

To validate that our cell line models and data are applicable to human lung cancer tissues, we conducted a mass spectrometry tyrosine phosphoproteomics analysis on four NSCLC tumor samples with TKI-sensitive *EGFR* mutations. In total, we identified 279 unique pTyr sites corresponding to 189 unique proteins across all four tumor samples. For each tumor, we identified 158, 153, 157, and 109 unique

Published OnlineFirst June 11, 2014; DOI: 10.1158/1078-0432.CCR-13-1559

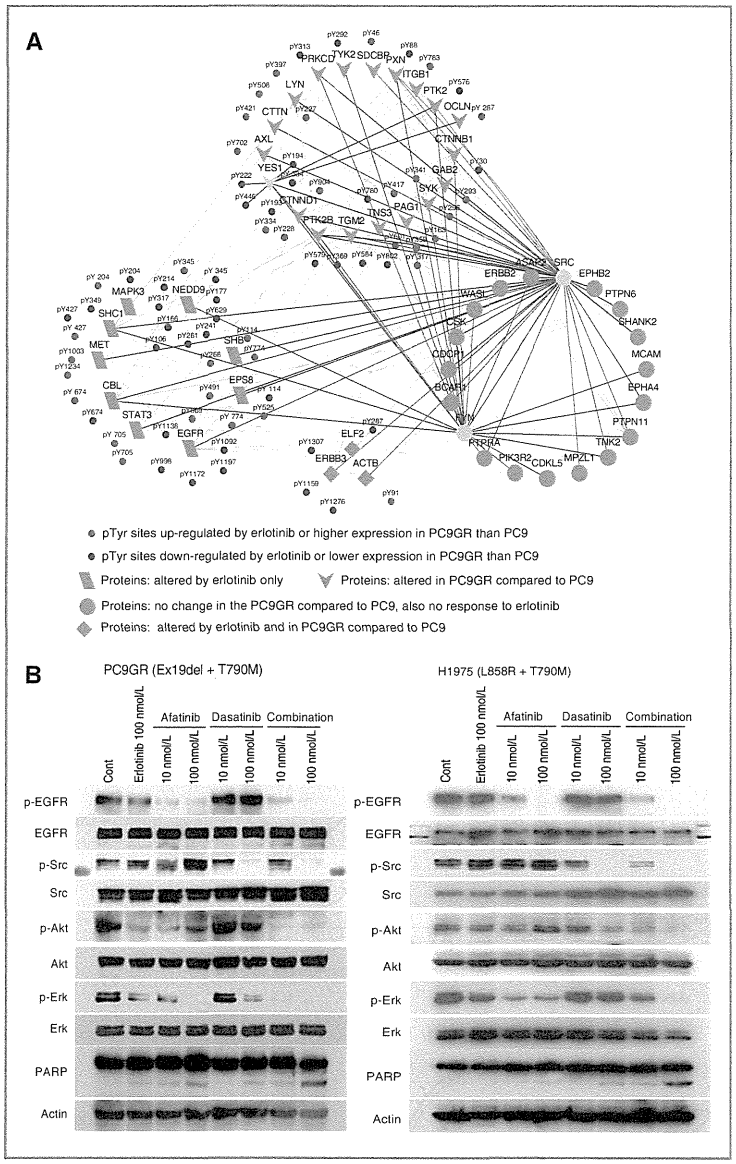

Figure 4. Effects of dasatinib combined with afatinib on EGFR signaling and cell growth in gefitinib-resistant NSCLC cells with T790M. A, pTyr proteins corresponding to pTyr peptides identified in PC9 and PC9GR cells are linked to SFK using InnateDB to capture literature reports and displayed in Cytoscape. Pink circle, pTyr sites upregulated by erlotinib or higher expression in PC9GR than in PC9 cells. Blue circle, pTyr sites downregulated by erlotinib or less expression in PC9GR than in PC9 cells. Yellow circles or V, SFK (SRC, YES1, FYN). Gray circle, pTyr proteins showing no difference between PC9 and PC9GR cells and no change with erlotinib treatment. Gray parallelogram, pTyr proteins altered by erlotinib across PC9 and PC9GR datasets. Gray V, pTyr proteins different between PC9 and PC9GR cells. Gray diamond, pTyr proteins different between PC9 and PC9GR cells and showing changes with erlotinib treatment. B, PC9GR and H1975 cells were incubated for 6 hours (or 24 hours for PARP) in the absence or presence of erlotinib (100 nmol/L), afatinib (10 and 100 nmol/L), dasatinib (10 and 100 nmol/L), or afatinib and dasatinib in combination (10 and 100 nmol/L), as indicated. Cell lysates were subjected to protein expression analysis with antibodies to pEGFR, EGFR, pAkt, Akt, pErk, Erk, pSrc family, Src, or PARP along with antibodies to β-actin as a loading control. (*Continued on the following page.*)

pTyr sites corresponding to 117, 95, 111, and 87 proteins, respectively (Supplementary Table S4). Importantly, 83 unique pTyr sites on 65 proteins identified from mass spectrometry experiments in PC9 cells were also observed active in human patient tissues (Supplementary Fig. S11 and Supplementary Table S5). This included: EGFR (pTyr1172, 1197), MET (pTyr1234), SFKs including SRC (pTyr 419), FYN (pTyr 214, 420), LYN (pTyr 32, 193, 104, 397), YES1 (pTyr223, 426), MK01 (pTyr 187), MK03 (pTyr 204), STAT3 (pTyr 705), and AXL (pTyr 886). These results in human tumor tissues from patients with *EGFR* mutations well validate our findings gained from cell line model, suggesting the potential of clinical application of our findings in this study.

Activation of Src or MET in human lung tumor samples with T790M gatekeeper *EGFR* mutations

To validate that Src phosphorylation is indeed observed as a target in human NSCLC samples with T790M gatekeeper mutation, we examined the expression of phosphorylated Src (Tyr 416) in tumor samples with T790M using immunohistochemical staining. We found pSrc in all *EGFR* T790M-positive tissue specimens, including 2 paired samples of pre- and post-EGFR-TKI treatment, with

Published OnlineFirst June 11, 2014; DOI: 10.1158/1078-0432.CCR-13-1559

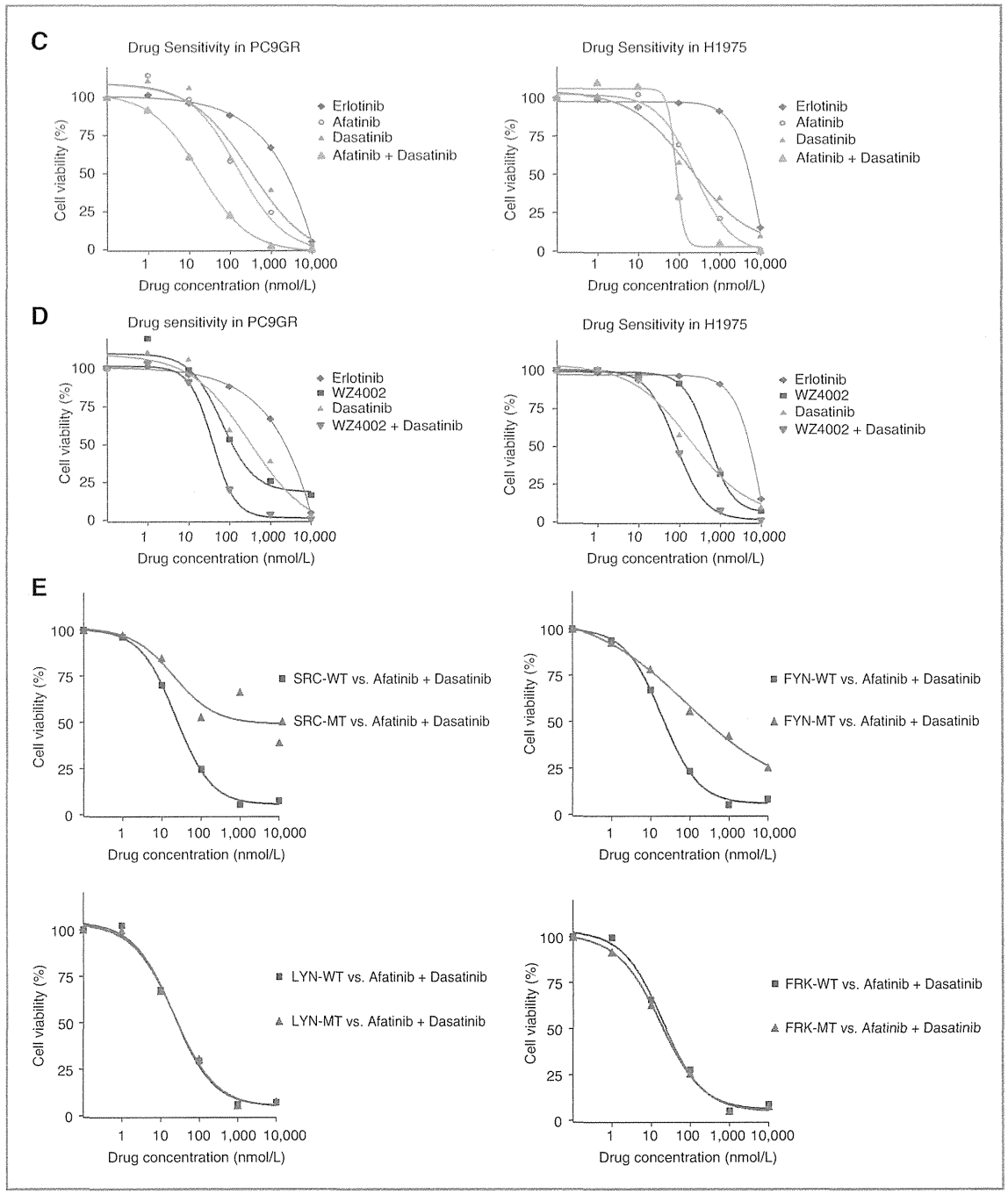

Figure 4. (*Continued.*) C, PC9GR and H1975 cells were treated for 72 hours with increasing concentrations of erlotinib alone, afatinib alone, dasatinib alone, or afatinib + dasatinib. D, PC9GR and H1975 cells were treated for 72 hours with increasing concentrations of erlotinib alone, WZ4002 alone, dasatinib alone, or WZ4002 + dasatinib. Data generated by cell viability assay (CellTiter-Glo) are expressed as a percentage of the value for untreated cells. Determinations were done in triplicate. E, PC9GR cells were infected with lentivirus expressing wild-type and mutant gatekeeper forms of each indicated Src family kinase for 48 hours. Subsequently, cells were exposed to increasing concentrations of afatinib plus dasatinib for 72 hours, after which cell viability was assessed by cell viability assay (CellTiter-Glo). Data are expressed as a percentage of the value for untreated cells. Determinations were done in triplicate. Please view online version for full details.

Published OnlineFirst June 11, 2014; DOI: 10.1158/1078-0432.CCR-13-1559

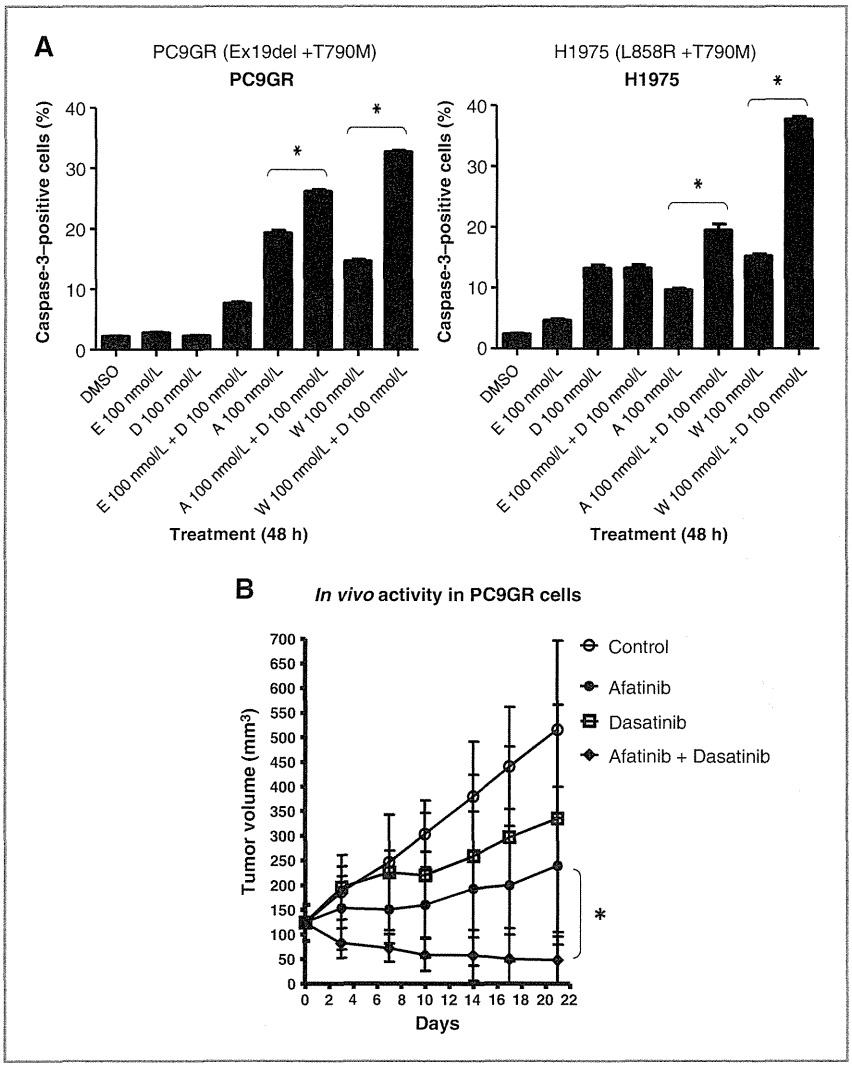

Figure 5. Effects of dasatinib combined with afatinib on apoptosis and *in vivo* tumor regression in gefitinib-resistant NSCLC cells with T790M. A, apoptosis assay was carried out using PE-conjugated caspase-3 antibody, following incubation of PC9GR or H1975 cells for 72 hours with DMSO, erlotinib (E), dasatinib (D), erlotinib + dasatinib, afatinib (A), afatinib + dasatinib, WZ4002 (W), and WZ4002 + dasatinib. Values are expressed as a percentage of caspase-3-positive cells. Determinations were done in triplicate. Bars, SD. *, $P < 0.001$ versus DMSO or each single agent (Student *t* test). B, Nude mice with tumor xenografts established by subcutaneous implantation of PC9GR cells were treated daily for 21 days with vehicle (control), afatinib (10 mg/kg), dasatinib (15 mg/kg), or afatinib + dasatinib by oral gavage. Tumor volume was determined at the indicated times after the onset of treatment. Points, mean of values from 5 mice/group; bars, SE. *, $P < 0.05$ for afatinib combined with dasatinib versus control or each agent alone by ANOVA (Tukey–Kramer comparison). (*Continued on the following page.*)

varied intensities and cellularity (Table 1; Fig. 5C). These results confirmed results from cell lines that Src activity persists in *EGFR* T790M-positive tumor tissues. We further examined changes in tyrosine phosphorylated MET expression in matched pre- and post-EGFR-TKI treatment patient tumor tissue specimens. We found evidence for increased tyrosine phosphorylated MET in one patient (patient 10 in Table 1) that was not due to increased total MET protein (Fig. 5D), whereas no evidence was found in the second patient (patient 9 in Table 1) for which pre- and posttreatment biopsy tissues were available for study. These results provide further support using tumor tissues that MET tyrosine phosphorylation can occur in T790M-containing tissues and this can be independent of total MET expression.

Discussion

We applied tyrosine phosphorylation profiling using LC/MS-MS to directly compare an EGFR-TKI–sensitive cell line versus its acquired resistance counterpart to uncover additional resistance mechanisms and propose cotargeting strategies to enhance the effects of agents specifically targeting the T790M EGFR allele. To our knowledge, this is the first such report to apply a mass spectrometry–based phosphoproteomics approach to compare the molecular networks between EGFR-TKI–sensitive and -resistant pairs. The driving force behind this approach is the limited efficacy of irreversible EGFR-TKIs in targeting T790M, as shown in both preclinical and clinical studies (8, 9, 12, 14–19), and the ability of

Published OnlineFirst June 11, 2014; DOI: 10.1158/1078-0432.CCR-13-1559

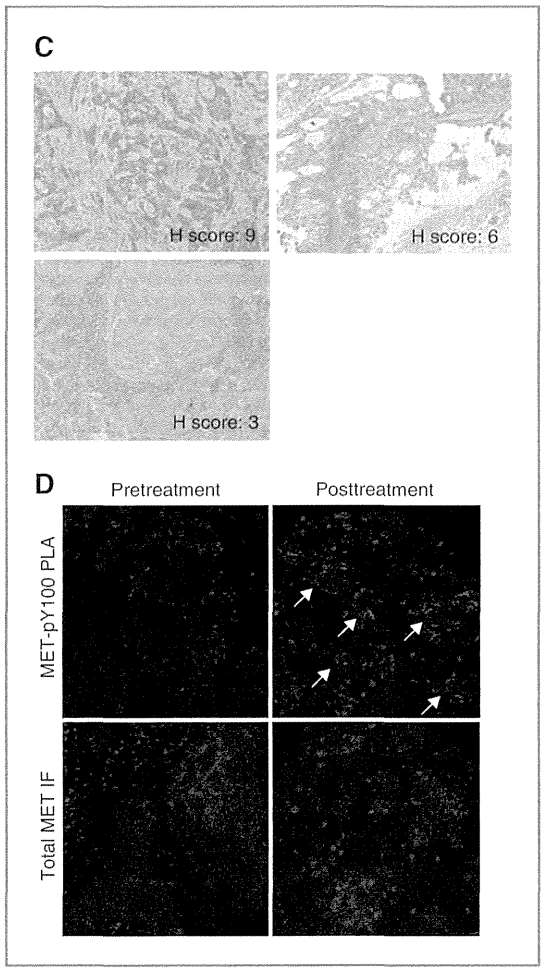

Figure 5. (*Continued.*) C, evidence for activation of Src in the T790M-positive biopsy specimens. Immunohistochemical staining was used to detect expression of tyrosine phosphorylation Src (Tyr416) in 10 EGFR T790M-positive tissue specimens. H score (intensity × cellularity) was calculated for each sample, with scores 0 and 9 representing the lowest and highest expression, respectively. Three representative ×200 images show the different levels of pSrc expression in EGFR T790M-positive human lung specimen. D, evidence for increased MET tyrosine phosphorylation in posttreatment T790M biopsy specimens. Proximity ligation assays (PLA) for MET and pY100 were performed to assess MET phosphorylation in serial biopsy specimens obtained from an adenocarcinoma patient (right lung, lower lobe, 33 months apart). Original biopsy confirmed *EGFR* exon21 L858R mutation; rebiopsy confirmed L858R/T790M mutation. Top, evidence of MET-pY PLA signal in pretreatment biopsy, while clusters of highly phosphorylated MET are observed in the posttreatment biopsy. MET-pY PLA was localized to cytokeratin (+)-staining regions (data not shown). Bottom, increased MET-pY PLA signal is not due to increased total MET protein.

other tyrosine kinases, especially RTKs, to limit EGFR-TKI efficacy. Through a systematic interrogation of pTyr peptides and proteins using LC/MS-MS, we identified both RTKs and non-RTKs able to be recruited to confer erlotinib sensitivity. In PC9GR cells, we identified higher levels of pTyr peptides corresponding to MET signaling, including more MET, ROR1, and Gab1/2 proteins. Interestingly, this coordinated activation of MET signaling was not secondary to *MET* gene amplification, as our FISH results revealed no amplification of the *MET* gene. The results with the basal phosphoproteome corresponded to HGF's strong effects in protecting both PC9 and PC9GR cells from erlotinib or afatinib, respectively. In addition, these results suggest a form of "lineage" addiction, whereby resistant cells with T790M can carry forward RTKs that can cooperate to drive resistance. Importantly, these results suggest that interrogating protein activation status or network signaling may highlight proteins that play a role in protecting cells against EGFR-TKI, especially when in a microenvironment rich with cognate growth factor ligands. Despite observing more AXL pTyr peptides in PC9GR cells, we demonstrated no ability of AXL pathway activation by Gas6 ligand to drive resistance to either erlotinib or afatinib. The reasons for this are not clear, but one limit of our approach was the lack of absolute measurements of pTyr peptides. It is possible that, compared with MET or IRS2 pTyr peptides, pTyr peptides corresponding to AXL are far lower in absolute amount and thus are inefficient to compete for downstream signaling effectors. It will be interesting and important to determine how basal phosphoproteome measurements can predict the effects of growth factor protection against targeted agents. As AXL signaling still remains poorly understood, another explanation for our results could be the limited or absence of key adaptors or other effector proteins involved in AXL signaling.

Using pTyr peptide data obtained from both PC9 and PC9GR cells exposed to erlotinib, we identified proteins downstream of EGFR in these cells with mutant gain-of-function EGFR proteins. One of the more interesting findings was that nearly half of the statistically significant pTyr peptides were increased in abundance following erlotinib treatment. It is increasingly recognized that signaling pathways display large amounts of crosstalk and that adaptive resistance mechanisms have been observed in cells exposed to targeted agents (41). Our results match our investigations using purified Src homology-2 domains to profile tyrosine kinase signaling in lung cancer cells, where we observed increased pTyr signaling in multiple lung cancer cells exposed to TKIs (42). Similar events have also been observed in crizotinib-treated EML4-ALK cells and dasatinib-treated DDR2-mutant lung cancer cells, arguing that these paradoxical changes are consistent across multiple tumor types and kinase inhibitors (unpublished observations). The underlying mechanisms of these changes require additional study, as they could be important in promoting adaptive resistance to targeted agents and could in some cases cooperate with microenvironmental factors, such as growth factors, to limit TKI efficacy. Collectively, these results suggest that cell intrinsic (receptors, signaling proteins) and extrinsic (ligands) factors can collaborate

Published OnlineFirst June 11, 2014; DOI: 10.1158/1078-0432.CCR-13-1559

Table 1. Src phosphorylation detected in human NSCLC samples with T790M gatekeeper mutation

Patient ID	EGFR mutant	H score	Intensity	Cellularity
1	T790M/L858R	3	1	3
2	T790M/19del(E746-A750)	4	2	2
3	T790M/19del(E746-A750)	6	2	3
4	T790M/L858R	6	2	3
5	T790M/19del(E746-A750)	6	2	3
6	T790M/19del(E746-A750)	9	3	3
7	T790M/19del(E746-A750)	9	3	3
8	T790M/L858R	9	3	3
9 (Pre-TKI)	19del(E746-A750)	9	3	3
9 (Post-TKI)	T790M/19del(E746-A750)	9	3	3
10 (Pre-TKI)	L858R	4	2	2
10 (Post-TKI)	T790M/L858R	9	3	3

NOTE: Patient 9 was treated with "gefitinib and erlotinib." Patient 10 was treated with "gefitinib and erlotinib + ARQ197 (MET-TKI)."

to drive resistance to kinase inhibitors in a systems-level manner.

Our phosphoproteomics analyses in PC9 and PC9GR cells demonstrated that SFKs are also critical as an EGFR-independent cosignal in NSCLC cells with T790M. These results were enabled by tyrosine phosphorylation profiling combined with analysis of proteins based on known protein–protein interactions. We validated the inferences derived from the phosphoproteomics by showing that afatinib combined with dasatinib resulted in antitumor activity regarding cell proliferation and apoptosis in PC9GR, H1975, HCC4006-T790M, and HCC827-T790M cells (each harboring T790M). These results appear to be generalized to additional T790M EGFR-TKIs, as dasatinib demonstrated similar combination effects with the T790M-selective EGFR-TKI WZ4002 (40). We did not observe combination effects with afatinib plus dasatinib compared with either agent alone in cells with TKI-sensitive *EGFR* mutation only (PC9, HCC4006, and HCC827 cells) or wild-type *EGFR* (H460, A549, and H1299 cells). The enhanced apoptosis with combined afatinib and dasatinib in the cells with T790M translated into improved *in vivo* effects on tumor growth in PC9GR cells. Collectively, our results suggest that dasatinib can be generally used as a combination therapy with irreversible or T790M-selective EGFR-TKIs for patients with NSCLC who acquired EGFR-TKI resistance associated with T790M.

As our approach was limited to examining the tyrosine phosphoproteome, we were unable to detect serine/threonine signaling including mTOR/AKT or MEK/Erk pathways both of which are also essential for carcinogenesis. Previous studies have indicated that mTOR inhibitor combined with MEK inhibitor or irreversible EGFR-TKI is potential strategy to overcome T790M (21, 43). Further studies examining the global phosphoproteome, such as with immobilized metal affinity chromatography which can detect serine/threonine phosphopeptides (44), could identify other proteins and pathways that may play roles in EGFR TKI resistance.

Although single-agent dasatinib has no activity in patients with NSCLC with TKI-sensitive *EGFR* mutation who acquired resistance to EGFR-TKI (45), our results suggest a role for SFKs in maintaining downstream signaling despite irreversible EGFR-TKIs and support further studies of irreversible EGFR-TKIs combined with dasatinib in patients with NSCLC who acquire resistance to EGFR-TKI. Src is known to be both an upstream activator and a downstream mediator of EGFR, and its phosphorylation is detected in about one-third of lung cancer tumors (46, 47). Although MET activation might not be always observed in the presence of T790M based on our *in vitro* and tumor tissue analysis, pSrc seems to be generally detected in our NSCLC tumor samples harboring T790M, consistent with our results of cell models. In addition, our mass spectrometry data from tumor samples with TKI-sensitive *EGFR* mutation demonstrated a high degree of overlap with results from cell models, thereby validating the overall approach. These results from tumor samples suggest that our results from lung cancer cell line models are applicable to translate in to the clinic. Our previous chemical and phosphoproteomic characterization identified nearly 40 different kinase targets of dasatinib and showed that SRC, FYN, and EGFR are relevant targets for dasatinib action in NSCLC (32). Our recent phase I/II study showed that dasatinib combined with erlotinib is tolerable, with 63% of patients with advanced NSCLC showing disease control, including two having partial response and one having bone response (48). Another group also showed that dasatinib combined with erlotinib is safe and feasible in NSCLC (49).

On the basis of these clinical studies along with the experiments reported here, dasatinib has potential clinical activity in NSCLC treatment, but this is limited to

Published OnlineFirst June 11, 2014; DOI: 10.1158/1078-0432.CCR-13-1559

combinations with T790M-targeted agents and in genotype-specific patients. This will be formally tested in a phase I trial of afatinib and dasatinib (NCT01999985). Our results also highlight the ability of phosphoproteomics to identify other important mediators of drug sensitivity, and examination of these proteins may be important in clinical studies of T790M-targeting agents.

Disclosure of Potential Conflicts of Interest

E.B. Haura reports receiving a commercial research grant from Boehringer-Ingelheim. No potential conflicts of interest were disclosed by the other authors.

Authors' Contributions

Conception and design: T. Yoshida, G. Zhang, E.B. Haura
Development of methodology: T. Yoshida, G. Zhang, M.A. Smith, A.S. Lopez, Y. Bai, J. Koomen, E.B. Haura
Acquisition of data (provided animals, acquired and managed patients, provided facilities, etc.): T. Yoshida, G. Zhang, M.A. Smith, B. Fang, J. Koomen, K. Nakagawa, E.B. Haura
Analysis and interpretation of data (e.g., statistical analysis, biostatistics, computational analysis): G. Zhang, M.A. Smith, A.S. Lopez, Y. Bai, B. Fang, B. Rawal, K.J. Fisher, A.Y. Chen, I. Okamoto, K. Nakagawa, E.B. Haura
Writing, review, and/or revision of the manuscript: T. Yoshida, G. Zhang, M.A. Smith, B. Fang, J. Koomen, B. Rawal, A.Y. Chen, K. Nakagawa, E.B. Haura
Administrative, technical, or material support (i.e., reporting or organizing data, constructing databases): T. Yoshida, G. Zhang, M.A. Smith, A.S. Lopez, Y. Bai, J. Li, M. Kitano, Y. Morita, H. Yamaguchi, K. Shibata, T. Okabe, I. Okamoto, K. Nakagawa, E.B. Haura
Study supervision: K. Nakagawa, E.B. Haura

Acknowledgments

The authors thank the Moffitt pY Group, the Kinki University Medical Oncology Research Group, Tsutomu Iwasa, and Kunio Okamoto for helpful discussions, Rasa Hamilton for editorial assistance, Fumi Kinose for assistance with cell culture, and Linda Ley and Carol Ulge for administrative assistance. The authors also thank BML, Inc and SRL, Inc for technical assistance.

Grant Support

The work was partially funded by grants from the Moffitt Cancer Center SPORE in Lung Cancer (P50-CA119997), the V Foundation for Cancer Research, and in part by the National Cancer Institute, part of the NIH, through grant number 2 P30-CA76292-14, which provide support to the Proteomics Core, the Flow Cytometry Core, the Tissue Core, and the Animal Facility at the H. Lee Moffitt Cancer Center and Research Institute, an NCI-designated Comprehensive Cancer Center.

The costs of publication of this article were defrayed in part by the payment of page charges. This article must therefore be hereby marked *advertisement* in accordance with 18 U.S.C. Section 1734 solely to indicate this fact.

Received June 13, 2013; revised April 9, 2014; accepted April 23, 2014; published OnlineFirst June 11, 2014.

References

1. Mok TS, Wu YL, Thongprasert S, Yang CH, Chu DT, Saijo N, et al. Gefitinib or carboplatin-paclitaxel in pulmonary adenocarcinoma. N Engl J Med 2009;361:947–57.
2. Mitsudomi T, Morita S, Yatabe Y, Negoro S, Okamoto I, Tsurutani J, et al. Gefitinib versus cisplatin plus docetaxel in patients with non-small-cell lung cancer harbouring mutations of the epidermal growth factor receptor (WJTOG3405): an open label, randomised phase 3 trial. Lancet Oncol 2010;11:121–8.
3. Kobayashi S, Boggon TJ, Dayaram T, Janne PA, Kocher O, Meyerson M, et al. EGFR mutation and resistance of non-small-cell lung cancer to gefitinib. N Engl J Med 2005;352:786–92.
4. Pao W, Miller VA, Politi KA, Riely GJ, Somwar R, Zakowski MF, et al. Acquired resistance of lung adenocarcinomas to gefitinib or erlotinib is associated with a second mutation in the EGFR kinase domain. PLoS Med 2005;2:e73.
5. Kosaka T, Yatabe Y, Endoh H, Yoshida K, Hida T, Tsuboi M, et al. Analysis of epidermal growth factor receptor gene mutation in patients with non-small cell lung cancer and acquired resistance to gefitinib. Clin Cancer Res 2006;12:5764–9.
6. Sequist LV, Waltman BA, Dias-Santagata D, Digumarthy S, Turke AB, Fidias P, et al. Genotypic and histological evolution of lung cancers acquiring resistance to EGFR inhibitors. Sci Transl Med 2011;3:75ra26.
7. Yu HA, Arcila ME, Rekhtman N, Sima CS, Zakowski MF, Pao W, et al. Analysis of tumor specimens at the time of acquired resistance to EGFR-TKI therapy in 155 patients with EGFR-mutant lung cancers. Clin Cancer Res 2013;19:2240–7.
8. Engelman JA, Mukohara T, Zejnullahu K, Lifshits E, Borras AM, Gale CM, et al. Allelic dilution obscures detection of a biologically significant resistance mutation in EGFR-amplified lung cancer. J Clin Invest 2006;116:2695–706.
9. Engelman JA, Zejnullahu K, Gale CM, Lifshits E, Gonzales AJ, Shimamura T, et al. PF00299804, an irreversible pan-ERBB inhibitor, is effective in lung cancer models with EGFR and ERBB2 mutations that are resistant to gefitinib. Cancer Res 2007;67:11924–32.
10. Li D, Ambrogio L, Shimamura T, Kubo S, Takahashi M, Chirieac LR, et al. BIBW2992, an irreversible EGFR/HER2 inhibitor highly effective in preclinical lung cancer models. Oncogene 2008;27:4702–11.
11. Kwak EL, Sordella R, Bell DW, Godin-Heymann N, Okimoto RA, Brannigan BW, et al. Irreversible inhibitors of the EGF receptor may circumvent acquired resistance to gefitinib. Proc Natl Acad Sci U S A 2005;102:7665–70.
12. Sos ML, Rode HB, Heynck S, Peifer M, Fischer F, Kluter S, et al. Chemogenomic profiling provides insights into the limited activity of irreversible EGFR inhibitors in tumor cells expressing the T790M EGFR resistance mutation. Cancer Res 2010;70:868–74.
13. Yun CH, Mengwasser KE, Toms AV, Woo MS, Greulich H, Wong KK, et al. The T790M mutation in EGFR kinase causes drug resistance by increasing the affinity for ATP. Proc Natl Acad Sci U S A 2008;105:2070–5.
14. Yu Z, Boggon TJ, Kobayashi S, Jin C, Ma PC, Dowlati A, et al. Resistance to an irreversible epidermal growth factor receptor (EGFR) inhibitor in EGFR-mutant lung cancer reveals novel treatment strategies. Cancer Res 2007;67:10417–27.
15. Godin-Heymann N, Ulkus L, Brannigan BW, McDermott U, Lamb J, Maheswaran S, et al. The T790M "gatekeeper" mutation in EGFR mediates resistance to low concentrations of an irreversible EGFR inhibitor. Mol Cancer Ther 2008;7:874–9.
16. Shimamura T, Li D, Ji H, Haringsma HJ, Liniker E, Borgman CL, et al. Hsp90 inhibition suppresses mutant EGFR-T790M signaling and overcomes kinase inhibitor resistance. Cancer Res 2008;68:5827–38.
17. Yamada T, Matsumoto K, Wang W, Li Q, Nishioka Y, Sekido Y, et al. Hepatocyte growth factor reduces susceptibility to an irreversible epidermal growth factor receptor inhibitor in EGFR-T790M mutant lung cancer. Clin Cancer Res 2010;16:174–83.
18. Ercan D, Zejnullahu K, Yonesaka K, Xiao Y, Capelletti M, Rogers A, et al. Amplification of EGFR T790M causes resistance to an irreversible EGFR inhibitor. Oncogene 2010;29:2346–56.
19. Miller VA, Hirsh V, Cadranel J, Chen YM, Park K, Kim SW, et al. Afatinib versus placebo for patients with advanced, metastatic non-small-cell lung cancer after failure of erlotinib, gefitinib, or both, and one or two lines of chemotherapy (LUX-Lung 1): a phase 2b/3 randomised trial. Lancet Oncol 2012;13:528–38.
20. Regales L, Gong Y, Shen R, de Stanchina E, Vivanco I, Goel A, et al. Dual targeting of EGFR can overcome a major drug resistance

Published OnlineFirst June 11, 2014; DOI: 10.1158/1078-0432.CCR-13-1559

mutation in mouse models of EGFR mutant lung cancer. J Clin Invest 2009;119:3000–10.
21. Li D, Shimamura T, Ji H, Chen L, Haringsma HJ, McNamara K, et al. Bronchial and peripheral murine lung carcinomas induced by T790M-L858R mutant EGFR respond to HKI-272 and rapamycin combination therapy. Cancer Cell 2007;12:81–93.
22. Stommel JM, Kimmelman AC, Ying H, Nabioullin R, Ponugoti AH, Wiedemeyer R, et al. Coactivation of receptor tyrosine kinases affects the response of tumor cells to targeted therapies. Science 2007;318:287–90.
23. Wilson TR, Fridlyand J, Yan Y, Penuel E, Burton L, Chan E, et al. Widespread potential for growth-factor-driven resistance to anticancer kinase inhibitors. Nature 2012;487:505–9.
24. Harbinski F, Craig VJ, Sanghavi S, Jeffery D, Liu L, Sheppard KA, et al. Rescue screens with secreted proteins reveal compensatory potential of receptor tyrosine kinases in driving cancer growth. Cancer Discov 2012;2:948–59.
25. Yano S, Wang W, Li Q, Matsumoto K, Sakurama H, Nakamura T, et al. Hepatocyte growth factor induces gefitinib resistance of lung adenocarcinoma with epidermal growth factor receptor-activating mutations. Cancer Res 2008;68:9479–87.
26. Machida K, Eschrich S, Li J, Bai Y, Koomen J, Mayer BJ, et al. Characterizing tyrosine phosphorylation signaling in lung cancer using SH2 profiling. PLoS ONE 2010;5:e13470.
27. Naoki K, Soejima K, Okamoto H, Hamamoto J, Hida N, Nakachi I, et al. The PCR-invader method (structure-specific 5′ nuclease-based method), a sensitive method for detecting EGFR gene mutations in lung cancer specimens; comparison with direct sequencing. Int J Clin Oncol 2011;16:335–44.
28. Engelman JA, Zejnullahu K, Mitsudomi T, Song Y, Hyland C, Park JO, et al. MET amplification leads to gefitinib resistance in lung cancer by activating ERBB3 signaling. Science 2007;316:1039–43.
29. Zhang G, Fang B, Liu RZ, Lin H, Kinose F, Bai Y, et al. Mass spectrometry mapping of epidermal growth factor receptor phosphorylation related to oncogenic mutations and tyrosine kinase inhibitor sensitivity. J Proteome Res 2011;10:305–19.
30. Lynn DJ, Winsor GL, Chan C, Richard N, Laird MR, Barsky A, et al. InnateDB: facilitating systems-level analyses of the mammalian innate immune response. Mol Syst Biol 2008;4:218.
31. Saito R, Smoot ME, Ono K, Ruscheinski J, Wang PL, Lotia S, et al. A travel guide to Cytoscape plugins. Nat Methods 2012;9:1069–76.
32. Li J, Rix U, Fang B, Bai Y, Edwards A, Colinge J, et al. A chemical and phosphoproteomic characterization of dasatinib action in lung cancer. Nat Chem Biol 2010;6:291–9.
33. Ogino A, Kitao H, Hirano S, Uchida A, Ishiai M, Kozuki T, et al. Emergence of epidermal growth factor receptor T790M mutation during chronic exposure to gefitinib in a non small cell lung cancer cell line. Cancer Res 2007;67:7807–14.
34. Rush J, Moritz A, Lee KA, Guo A, Goss VL, Spek EJ, et al. Immunoaffinity profiling of tyrosine phosphorylation in cancer cells. Nat Biotechnol 2005;23:94–101.
35. Gentile A, Lazzari L, Benvenuti S, Trusolino L, Comoglio PM. Ror1 is a pseudokinase that is crucial for Met-driven tumorigenesis. Cancer Res 2011;71:3132–41.
36. Zhang Z, Lee JC, Lin L, Olivas V, Au V, LaFramboise T, et al. Activation of the AXL kinase causes resistance to EGFR-targeted therapy in lung cancer. Nat Genet 2012;44:852–60.
37. Komiyama NH, Watabe AM, Carlisle HJ, Porter K, Charlesworth P, Monti J, et al. SynGAP regulates ERK/MAPK signaling, synaptic plasticity, and learning in the complex with postsynaptic density 95 and NMDA receptor. J Neurosci 2002;22:9721–32.
38. Rumbaugh G, Adams JP, Kim JH, Huganir RL. SynGAP regulates synaptic strength and mitogen-activated protein kinases in cultured neurons. Proc Natl Acad Sci U S A 2006;103:4344–51.
39. Cantalupo G, Alifano P, Roberti V, Bruni CB, Bucci C. Rab-interacting lysosomal protein (RILP): the Rab7 effector required for transport to lysosomes. EMBO J 2001;20:683–93.
40. Zhou W, Ercan D, Chen L, Yun CH, Li D, Capelletti M, et al. Novel mutant-selective EGFR kinase inhibitors against EGFR T790M. Nature 2009;462:1070–4.
41. Chandarlapaty S. Negative feedback and adaptive resistance to the targeted therapy of cancer. Cancer Discov 2012;2:311–9.
42. Machida K, Thompson CM, Dierck K, Jablonowski K, Karkkainen S, Liu B, et al. High-throughput phosphotyrosine profiling using SH2 domains. Mol Cell 2007;26:899–915.
43. Faber AC, Li D, Song Y, Liang MC, Yeap BY, Bronson RT, et al. Differential induction of apoptosis in HER2 and EGFR addicted cancers following PI3K inhibition. Proc Natl Acad Sci U S A 2009;106:19503–8.
44. Kim JY, Welsh EA, Oguz U, Fang B, Bai Y, Kinose F, et al. Dissection of TBK1 signaling via phosphoproteomics in lung cancer cells. Proc Natl Acad Sci U S A 2013;110:12414–9.
45. Johnson ML, Riely GJ, Rizvi NA, Azzoli CG, Kris MG, Sima CS, et al. Phase II trial of dasatinib for patients with acquired resistance to treatment with the epidermal growth factor receptor tyrosine kinase inhibitors erlotinib or gefitinib. J Thorac Oncol 2011;6:1128–31.
46. Zhang J, Kalyankrishna S, Wislez M, Thilaganathan N, Saigal B, Wei W, et al. SRC-family kinases are activated in non-small cell lung cancer and promote the survival of epidermal growth factor receptor-dependent cell lines. Am J Pathol 2007;170:366–76.
47. Leung EL, Tam IY, Tin VP, Chua DT, Sihoe AD, Cheng LC, et al. SRC promotes survival and invasion of lung cancers with epidermal growth factor receptor abnormalities and is a potential candidate for molecular-targeted therapy. Mol Cancer Res 2009;7:923–32.
48. Haura EB, Tanvetyanon T, Chiappori A, Williams C, Simon G, Antonia S, et al. Phase I/II study of the Src inhibitor dasatinib in combination with erlotinib in advanced non-small-cell lung cancer. J Clin Oncol 2010;28:1387–94.
49. Johnson FM, Tang X, Tran HT, McIntyre C, Price J, Lee JJ, et al. A phase I/II study combining dasatinib (D) and erlotinib (E) in non-small cell lung cancer. J Clin Oncol 31, 2013 (suppl; abstr 8102).

Published OnlineFirst June 11, 2014; DOI: 10.1158/1078-0432.CCR-13-1559

AACR American Association for Cancer Research

Clinical Cancer Research

Tyrosine Phosphoproteomics Identifies Both Codrivers and Cotargeting Strategies for T790M-Related EGFR-TKI Resistance in Non–Small Cell Lung Cancer

Takeshi Yoshida, Guolin Zhang, Matthew A. Smith, et al.

Clin Cancer Res 2014;20:4059-4074. Published OnlineFirst June 11, 2014.

Cancers **2014**, *6*, 1540-1552; doi:10.3390/cancers6031540

OPEN ACCESS

cancers

ISSN 2072-6694

www.mdpi.com/journal/cancers

Review

Targeting *MET* Amplification as a New Oncogenic Driver

Hisato Kawakami [1], Isamu Okamoto [1,2,*], Wataru Okamoto [1,3], Junko Tanizaki [1,4], Kazuhiko Nakagawa [1] and Kazuto Nishio [5]

[1] Department of Medical Oncology, Kinki University Faculty of Medicine, 377-2 Ohno-higashi, Osaka-Sayama, Osaka 589-8511, Japan; E-Mails: kawakami_h@dotd.med.kindai.ac.jp (H.K.); wokamoto@east.ncc.go.jp (W.O.); Junko_Tanizaki@dfci.harvard.edu (J.T.); nakagawa@med.kindai.ac.jp (K.N.)

[2] Center for Clinical and Translational Research, Kyushu University Hospital, 3-1-1 Maidashi, Higashiku, Fukuoka 812-8582, Japan

[3] Division of Translational Research, Exploratory Oncology Research & Clinical Trial Center, National Cancer Center, 6-5-1 Kashiwanoha, Kashiwa, Chiba 277-8577, Japan

[4] Lowe Center for Thoracic Oncology, Dana-Farber Cancer Institute, HIM223, 450 Brookline Avenue, Boston, MA 02215, USA

[5] Department of Genome Biology, Kinki University Faculty of Medicine, 377-2 Ohno-higashi, Osaka-Sayama, Osaka 589-8511, Japan; E-Mail: knishio@med.kindai.ac.jp

* Author to whom correspondence should be addressed; E-Mail: okamotoi@kokyu.med.kyushu-u.ac.jp; Tel.: +81-92-642-5378; Fax: +81-92-642-5390.

Received: 21 May 2014; in revised form: 13 July 2014 / Accepted: 15 July 2014 / Published: 22 July 2014

Abstract: Certain genetically defined cancers are dependent on a single overactive oncogene for their proliferation and survival, a phenomenon known as "oncogene addiction". A new generation of drugs that selectively target such "driver oncogenes" manifests a clinical efficacy greater than that of conventional chemotherapy in appropriate genetically defined patients. *MET* is a proto-oncogene that encodes a receptor tyrosine kinase, and aberrant activation of MET signaling occurs in a subset of advanced cancers as result of various genetic alterations including gene amplification, polysomy, and gene mutation. Our preclinical studies have shown that inhibition of MET signaling either with the small-molecule MET inhibitor crizotinib or by RNA interference targeted to MET mRNA resulted in marked antitumor effects in cancer cell lines with *MET* amplification both *in vitro* and *in vivo*. Furthermore, patients with non-small cell lung cancer or gastric cancer positive for *MET* amplification have shown a pronounced clinical response to crizotinib. Accumulating

preclinical and clinical evidence thus suggests that *MET* amplification is an "oncogenic driver" and therefore a valid target for treatment. However, the prevalence of *MET* amplification has not been fully determined, possibly in part because of the difficulty in evaluating gene amplification. In this review, we provide a rationale for targeting this genetic alteration in cancer therapy.

Keywords: MET; gene amplification; non-small cell lung cancer; gastric cancer; fluorescence in situ hybridization (FISH); polymerase chain reaction (PCR); crizotinib

1. Introduction

Certain genetically defined cancers are dependent on a single overactive oncogene for their proliferation and survival, a phenomenon known as "oncogene addiction" that is exemplified by the *BCR-ABL* fusion gene in chronic myeloid leukemia as well as by mutant forms of the epidermal growth factor receptor (EGFR) gene and by the *EML4-ALK* fusion gene in non-small cell lung cancer (NSCLC). A new generation of drugs that selectively target such "driver oncogenes" and which include tyrosine kinase inhibitors (TKIs) has shown a therapeutic efficacy greater than that of conventional chemotherapy in individuals with these specific molecular alterations [1,2]. The identification of additional kinase oncogenes would thus be expected to facilitate the development of new molecularly targeted therapies.

The proto-oncogene *MET* encodes the receptor tyrosine kinase c-MET (or MET). The binding of its ligand—the hepatocyte growth factor (HGF)—to MET results in tyrosine phosphorylation of the receptor and activation of downstream signaling pathways mediated by phosphoinositide 3-kinase (PI3K) and AKT, by signal transducer and activator of transcription 3 (STAT3), or by RAS and mitogen-activated protein kinase (MAPK). Whereas normal activation of MET is essential for wound healing and embryonic development [3,4], excessive activation of MET signaling in a subset of advanced cancers [5–9] results in the up-regulation of cell proliferation, motility, migration, and invasion [3,10]. Although such aberrant MET signaling potentially arises from genetic alteration or dysregulation of *MET* [11], the target potential of *MET* alterations including polysomy, gene amplification, and gene mutation has not been well established.

2. Preclinical Findings

To investigate the biological impact of *MET* amplification or mutation, we have examined the effects of a MET-TKI and of a small interfering RNA (siRNA) specific for MET mRNA on cell survival and signal transduction in NSCLC cells with or without such genetic alterations of *MET* [12]. Several types of *MET* mutation, including those that affect the kinase domain or other domains of the encoded protein, have been identified in tumors. The small-molecule drug crizotinib (PF-02341066) inhibits the tyrosine kinase activity of MET as well as that of oncogenic fusion variants of anaplastic lymphoma kinase (ALK) [13,14]. We found that inhibition of MET signaling with crizotinib or MET siRNA induced apoptosis that was accompanied by attenuation of the phosphorylation (activation) of AKT and the MAPK extracellular signal-regulated kinase (ERK) in NSCLC cells with *MET* amplification but not in

those positive for a non-kinase domain mutation (N375S or deletion of exon 14) of *MET* [12]. These results suggest that MET signaling is essential for the survival of NSCLC cells with *MET* amplification but not for that of those without this genetic alteration, including those with a non-kinase domain mutation of *MET*, although MET-TKIs have been shown to be active against MET with mutations in the kinase domain [15]. Crizotinib also showed a marked antitumor effect on lung cancer xenografts positive for *MET* amplification, whereas it had little effect on those negative for *MET* amplification, including those with a *MET* mutation, consistent with our results obtained *in vitro*. Together, these findings suggest that gene amplification, but not gene mutation, renders *MET* active as a driver oncogene.

In gastric cancer, in which gain-of-function mutations of *MET* are exceedingly rare [16–18], activation of *MET* has been attributed to gene amplification [19–21]. A highly selective MET-TKI, PHA-665752, was shown to have potential antitumor efficacy in gastric cancer cells with *MET* amplification [22]. We therefore also examined the potential antitumor action of crizotinib or MET siRNA in gastric cancer cells positive or negative for *MET* amplification [23]. Consistent with our results obtained with NSCLC cells [12], we found that inhibition of MET signaling by either of these agents resulted in induction of apoptosis associated with inhibition of AKT and ERK phosphorylation in gastric cancer cells with *MET* amplification but not in those without it, suggesting that MET signaling is essential for the survival of *MET* amplification-positive cells. Crizotinib also manifested a marked antitumor effect on gastric cancer xenografts positive for *MET* amplification, whereas it had little effect on those negative for this genetic change. Crizotinib thus showed a pronounced antitumor action both *in vitro* and *in vivo* specifically in gastric cancer cells positive for *MET* amplification.

In summary, our preclinical studies have shown that gene amplification, but not gene mutation, confers "oncogenic driver" potential on *MET*. Tumor cells positive for *MET* amplification are thus dependent on ("addicted to") sustained MET activity for their growth and survival, with the result that inhibition of MET signaling either with a small-molecule MET inhibitor or by RNA interference targeted to MET mRNA has marked antitumor effects both *in vitro* and *in vivo*. These findings provide a rationale for targeting *MET* amplification with MET-TKIs in the clinical setting.

3. Prevalence of *MET* Amplification in Cancer Patients

Given the potential of MET-targeted therapy for cancer with *MET* amplification, it is important to determine the prevalence of this gene alteration in patients with advanced cancer. Unfortunately, however, different studies have used different methods and criteria to detect *MET* amplification (Tables 1 and 2). Studies based on fluorescence *in situ* hybridization (FISH) analysis have identified *MET* amplification in up to ~5% of patients with NSCLC [24–27] or gastric cancer [20,28,29], whereas an increase in *MET* copy number was found in up to ~20% of NSCLC [30–35] and gastric cancer [36–40] patients by Southern blot analysis or with a polymerase chain reaction (PCR)-based assay. To understand the reason for this discrepancy, it is important to recognize the difference between the two genetic mechanisms—gene amplification and polysomy—that can give rise to an increase in gene copy number in malignant tumors. Gene amplification is defined as a copy number increase for a specific gene (or group of genes) on a given chromosome arm without a change in copy number for genes located in other regions of the chromosome [41]. On the other hand, polysomy gives rise to a copy number gain for a given gene as a result of the presence of extra copies of the entire chromosome. Of note, polysomy for

chromosome 7 (the chromosome on which *MET* is located) was indeed observed ~30% of NSCLC [27] and gastric [29] tumors with an increased *MET* copy number. Furthermore, such tumors might not be MET driven, given that breast tumors with an increased copy number for the human epidermal growth factor receptor 2 (HER2) gene as a result of polysomy 17 behave as HER2-negative tumors [42]. Southern blot analysis and PCR-based assays identify a gain in gene copy number regardless of the underlying cause and are thus unable to discriminate gene amplification from polysomy (Figure 1A). This methodological limitation is sometimes overlooked in determination of the prevalence of *MET* amplification in cancer.

Table 1. Prevalence of *MET* amplification and increased *MET* gene copy number (GCN) in NSCLC.

Study	Number of Patients	Technique	Classification	Positivity (%)
Camidge *et al.* (2010) [43]	66	FISH	*MET/CEP7* ratio > 2.0	0
Onozato *et al.* (2009) [33]	148	PCR based	GCN > 2	1.4
Kubo *et al.* (2009) [34]	100	PCR based	GCN > 5	2.0
Bean *et al.* (2007) [30]	16	PCR based	GCN > 5	3.0
Go *et al.* (2010) [27]	180	FISH	*MET/CEP7* ratio > 2.0	3.9
Okamoto *et al.* (2014) [44]	229	FISH	*MET/CEP7* ratio > 2.2	3.9
Cappuzzo *et al.* (2009) [45]	447	FISH	*MET/CEP7* ratio > 2.0	4.1
Onitsuka *et al.* (2010) [32]	183	PCR based	GCN > 1.31	4.4
Okuda *et al.* (2008) [31]	213	PCR based	GCN > 3	5.6
Beau-Faller *et al.* (2008) [35]	106	PCR based	GCN > mean + 2SD of 30 normal lung DNA samples	20.8

FISH, fluorescence in situ hybridization; PCR, polymerase chain reaction; GCN, gene copy number; CEP7, centromeric portion of chromosome 7.

Table 2. Prevalence of *MET* amplification and increased *MET* gene copy number (GCN) in gastric cancer.

Study	Number of Patients	Technique	Classification	Positivity (%)
Janjigian *et al.* (2011) [29]	38	FISH	*MET/CEP7* ratio > 2.0	0
Kawakami *et al.* (2013) [46]	266	FISH	*MET/CEP7* ratio > 2.2	1.5
Lennerz *et al.* (2011) [28]	267 (junctional and gastric)	FISH	*MET/CEP7* ratio > 2.2	2.2
Hara *et al.* (1998) [20]	154	FISH	NA	3.9
Liu *et al.* (2014) [47]	196	FISH	*MET/CEP7* ratio > 2.0	6.1
Graziano *et al.* (2011) [40]	216	PCR based	GCN ≥ 5	9.7
Tsugawa *et al.* (1998) [21]	70	Slot blot analysis	Ratio > 2 (relative to normal mucosa)	10.0
Nakajima *et al.* (1999) [19]	128	Southern blot analysis	Ratio > 2 (relative to normal mucosa)	10.2
Lee *et al.* (2011) [39]	472	PCR based	GCN ≥ 4	21.2
Shi *et al.* (2012) [48]	128	PCR based	GCN ≥ 4	30.5

FISH, fluorescence in situ hybridization; PCR, polymerase chain reaction; GCN, gene copy number; CEP7, centromeric portion of chromosome 7; NA, not available.

On the other hand, FISH analysis is a semiquantitative method that can be performed with two probes for determination of the number of signals both for a target gene and for the centromeric portion of the corresponding chromosome. Given that the number of centromeric signals directly indicates the copy number of the chromosome, FISH analysis reveals the copy number increase for the target gene from the ratio of the copy number of the gene to that of the chromosome (Figure 1). Comparative genomic hybridization (CGH) is another molecular cytogenetic approach to the identification of gene amplification. CGH analyzes copy number variation for whole chromosomes or subchromosomal regions relative to ploidy level in the DNA of a test sample in comparison with a reference sample [49]. Although CGH has proved to be an efficient and reproducible technique, it remains relatively expensive to perform and requires a well-equipped laboratory and a high level of operator expertise.

Figure 1. (**A**) Schematic comparison of gene amplification and polysomy. The ratio of the copy number for the target gene to that for the centromeric portion of the chromosome distinguishes an increased copy number of the target gene attributable to gene amplification from that resulting from extra copies of the chromosome (polysomy). (**B**) FISH analysis of a gastric cancer cell line (HSC58) positive for *MET* amplification. The image shows a single cancer cell, with green and red signals corresponding to *CEP7* (*CEN7p*) and the *MET* locus, respectively.

A

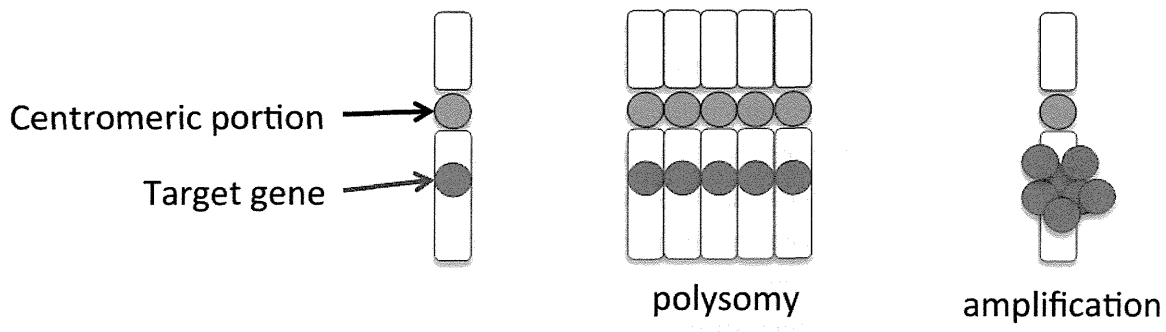

B

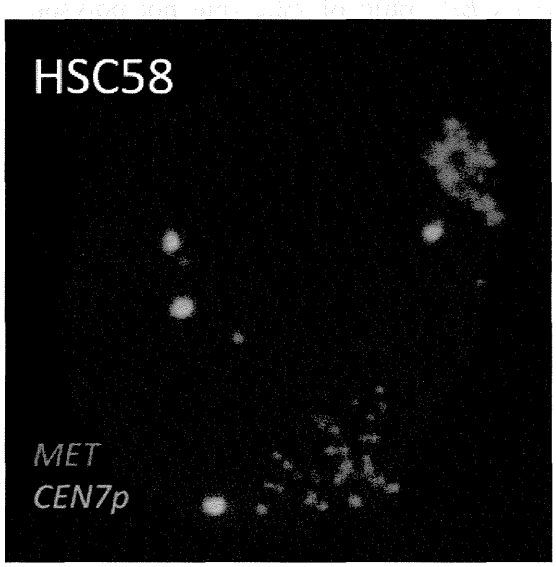

FISH is thus currently the gold standard for detection of gene amplification. According to the recent ASCO/CAP guidelines for *HER2* testing, gene amplification is defined as positive with a target gene/centromere ratio of >2.2, negative with a ratio of <1.8, and equivocal with a ratio between 1.8 and 2.2 [50]. Importantly, polysomy, which is mechanistically distinct from gene amplification, is mostly associated with a ratio in the equivocal range [51].

With the strict definition of *MET* amplification as a *MET/CEP7* (centromeric region of chromosome 7) ratio of >2.2 as determined by FISH analysis, we identified nine out of 229 patients with advanced NSCLC (3.9%) as being positive for *MET* amplification [44]. We also found that four out of 266 gastric cancer patients (1.5%) were positive for *MET* amplification as determined with a combination of PCR-based screening and FISH confirmation [46]. These results suggest that *MET* amplification identifies a small but clinically important subgroup of cancer patients who are likely to respond to MET-TKIs.

4. Clinical Response to Crizotinib in *MET* Amplification—Positive Cancer Patients

To date, at least 17 MET-TKIs with kinase selectivity profiles ranging from highly selective to multitargeted have been or are currently being subjected to clinical evaluation [52]. Although several agents including cabozantinib [53] and foretinib [54] have made good progress, they are multitargeted MET-TKIs, and so little is known of the relation between their efficacy and *MET* amplification. In NSCLC, *MET* amplification is one of the mechanisms responsible for the development of resistance to EGFR-TKIs, with dual inhibition of EGFR and MET having been shown to induce apoptosis in such resistant cells [55]. Combination treatment with an EGFR-TKI and tivantinib, a selective MET-TKI with microtubule-disrupting activity similar to that of vincristine [56], has been evaluated in clinical trials, but the efficacy of this approach remains unclear. Among the MET-TKIs examined, however, crizotinib has consistently shown efficacy in patients with cancer positive for *MET* amplification.

Preliminary reports of the clinical response of patients with *MET* amplification-positive cancer to crizotinib have come from an enriched molecular cohort of individuals with advanced cancer in a phase I trial of this drug (A8081001, ClinicalTrials.gov identifier NCT00585195). This cohort includes patients with various tumor types harboring specific genetic alterations of *MET* or *ALK*, including *MET* amplification defined as a *MET/CEP7* ratio of >2.2 (but not polysomy 7, kinase domain-activating mutations of *MET*, or other chromosomal translocations leading to altered transcriptional regulation of *MET*) as well as *ALK* chromosomal translocation or gene amplification. A patient with stage IV lung adenocarcinoma that was negative for *ALK* rearrangement but positive for high-level *MET* amplification (*MET/CEP7* ratio of >5.0) started treatment with crizotinib at a dose of 250 mg twice a day [57]. The patient achieved a maximum reduction in aggregate tumor measurement of 54.8% after 4 months of such therapy and thereafter continued the study treatment showing a partial response. A patient with *MET* amplification-positive glioblastoma was also treated with crizotinib at 250 mg twice a day [58]. After 2 months of treatment, the first scheduled cranial magnetic resonance imaging (MRI) scan revealed a 40% reduction in tumor size, and after 4 months a restaging cranial MRI examination confirmed this effect to be stable. Administration of crizotinib was continued for a total of 6 months, until the patient manifested disease progression.

Another study revealed a pronounced clinical response to crizotinib in two of four patients with gastric cancer positive for *MET* amplification (*MET/CEP7* ratio of >2.2) [28]. After 1 week of crizotinib